JCI insight

Stress responses, M2 macrophages, and a distinct microbial signature in fatal intestinal acute graft-versus-host disease

Shernan G. Holtan, … , Daniel J. Weisdorf, Jinhua Wang

JCI Insight. 2019. https://doi.org/10.1172/jci.insight.129762.

Research In-Press Preview **Inflammation** **Transplantation**

Steroid-refractory intestinal acute graft-versus-host disease (aGVHD) is a frequently fatal condition with little known about mechanisms driving failed steroid responses in gut mucosa. To uncover novel molecular insights in steroid-refractory aGVHD, we compared gene expression profiles of rectosigmoid biopsies from patients at diagnosis of clinical stage 3-4 lower intestinal aGVHD (N=22), to repeat biopsies when the patients became steroid refractory (N=22), and normal controls (N=10). We also performed single gene analyses of factors associated with tolerance (programmed death ligand-1 [*PDL1*], indoleamine 2,3 dioxygenase [IDO1], and T cell immunoreceptor with Ig and ITIM domains [*TIGIT*]) and found that significantly higher expression levels of these aGVHD inhibitory genes (*PDL1*, *IDO1*, *TIGIT*) at aGVHD onset became decreased in the steroid-refractory state. We examined genes triggered by microbial ligands to stimulate gut repair, amphiregulin (AREG) and the aryl hydrocarbon receptor (*AhR*), and found that both *AREG* and *AhR* gene expression levels were increased at aGVHD onset and remained elevated in steroid-refractory aGVHD. We also identified higher expression levels of metallothioneines, metal-binding enzymes induced in stress responses, and M2 macrophage genes in steroid-refractory aGVHD. We observed no differences in T-cell subsets between onset and steroid-refractory aGVHD. Patients with a rapidly fatal course showed greater DNA damage and a distinct microbial signature at aGVHD onset, whereas patients with more prolonged survival exhibited a gene expression profile […]

Stress responses, M2 macrophages, and a distinct microbial signature in fatal intestinal acute graft-versus-host disease

Shernan G. Holtan[1*], Ashraf Shabaneh[2*], Brian C. Betts[1], Armin Rashidi[1], Margaret L. MacMillan[3], Celalletin Ustun[4], Khalid Amin[5], Byron P. Vaughn[6], Justin Howard[6], Alexander Khoruts[6], Mukta Arora[1], Todd E. DeFor[7], Darrell Johnson[8], Bruce R. Blazar[3], Daniel J. Weisdorf[1], Jinhua Wang[9]

1. Blood and Marrow Transplant Program, Department of Medicine, University of Minnesota, Minneapolis, MN
2. Institute for Health Informatics, University of Minnesota
3. Blood and Marrow Transplant Program, Department of Pediatrics, University of Minnesota, Minneapolis, MN
4. Rush University Blood and Marrow Transplant Program, Chicago, IL
5. Department of Pathology, University of Minnesota
6. Division of Gastroenterology, Department of Medicine, University of Minnesota, Minneapolis, MN
7. Biostatistics, Masonic Cancer Center, University of Minnesota
8. Genomics Core Facility, University of Minnesota
9. Cancer Bioinformatics, Masonic Cancer Center, University of Minnesota

*Contributed equally

Running title: GI GVHD RNAseq

Corresponding author:
Shernan G. Holtan, MD
Assistant Professor of Medicine
Blood and Marrow Transplant Program
University of Minnesota
420 Delaware Street SE, MMC 480
Minneapolis, MN 55455
Phone: (612) 301-1095
Fax: (612) 625-6919
Email: sgholtan@umn.edu

Abstract: 245 words
Manuscript: 3377 words
Tables: 4
Figures: 7
Supplemental Figures: 3
References: 55

Key words: Allogeneic hematopoietic cell transplantation, acute GVHD, RNAseq
Disclaimers: The authors of this manuscript have no relevant conflicts of interest to disclose.

Abstract

Steroid-refractory intestinal acute graft-versus-host disease (aGVHD) is a frequently fatal condition with little known about mechanisms driving failed steroid responses in gut mucosa. To uncover novel molecular insights in steroid-refractory aGVHD, we compared gene expression profiles of rectosigmoid biopsies from patients at diagnosis of clinical stage 3-4 lower intestinal aGVHD (N=22), to repeat biopsies when the patients became steroid refractory (N=22), and normal controls (N=10). We also performed single gene analyses of factors associated with tolerance (programmed death ligand-1 [*PDL1*], indoleamine 2,3 dioxygenase [IDO1], and T cell immunoreceptor with Ig and ITIM domains [*TIGIT*]) and found that significantly higher expression levels of these aGVHD inhibitory genes (*PDL1*, *IDO1*, *TIGIT*) at aGVHD onset became decreased in the steroid-refractory state. We examined genes triggered by microbial ligands to stimulate gut repair, amphiregulin (AREG) and the aryl hydrocarbon receptor (*AhR*), and found that both *AREG* and *AhR* gene expression levels were increased at aGVHD onset and remained elevated in steroid-refractory aGVHD. We also identified higher expression levels of metallothioneines, metal-binding enzymes induced in stress responses, and M2 macrophage genes in steroid-refractory aGVHD. We observed no differences in T-cell subsets between onset and steroid-refractory aGVHD. Patients with a rapidly fatal course showed greater DNA damage and a distinct microbial signature at aGVHD onset, whereas patients with more prolonged survival exhibited a gene expression profile consistent with activation of *Smoothened*. Our results extend the paradigm beyond T cell-centric therapies for steroid-refractory GI aGVHD and highlight new mechanisms for therapeutic exploration.

Introduction

Patients with severe gastrointestinal (GI) acute graft-versus-host disease (aGVHD) who do not respond to steroids have a dismal prognosis. For decades, such patients have been treated with escalated immunosuppression based upon the clinical assumption that the donor T cells responsible for aGVHD are persistently damaging tissues despite high-dose steroids. Unfortunately, few patients with steroid-refractory aGVHD respond to escalated T-cell-targeted immunosuppression, and most ultimately succumb to unresolved organ damage or infection.(1, 2)

Little data derived from human GVHD target tissue samples exists to guide novel therapies in steroid-refractory aGVHD. Detailed histologic evaluation of GI aGVHD has demonstrated crypt loss, mucosal atrophy, and mucosal hemorrhage as potential hallmarks of severe aGVHD.(3-6) Inflammatory findings are often non-specific, providing little information as to the functional changes occurring in the tissue.(6) This paucity of target tissue biological data may have contributed to the relative lack of progress in therapy for steroid-refractory aGVHD for many years.

To uncover novel molecular insights driving fatal human steroid-refractory aGVHD, we performed ribonucleic acid sequencing (RNAseq) on archived formalin-fixed paraffin embedded (FFPE) rectosigmoid biopsies obtained during the routine clinical care of patients for diagnosis of lower GI stage 3-4 aGVHD at onset (N=22) compared to their repeat biopsies obtained for evaluation of steroid-refractory aGVHD. In doing so, we could identify transcriptomal changes in the severely affected intestinal mucosa when the patients' clinical status deteriorated due to apparent inadequate steroid response. We also compared aGVHD samples to 10 normal rectosigmoid biopsies to gain additional insight into the pathophysiology of life-threatening aGVHD itself, validating our findings using NanoString. Both microbial and human RNA are sequenced with RNAseq, and simultaneous analysis of host-microbe interactions is increasingly

feasible albeit largely limited to in vitro experiments to date.(7, 8) We analyzed microbial gene expression in our intestinal mucosa biopsies and noted a distinct profile in rapidly fatal aGVHD.

Results

Patient Descriptions and Outcomes

Patient demographics are detailed in Table 1. This is an adult population undergoing HCT for hematologic malignancy. The majority of patients were male (73%) and underwent reduced intensity conditioning (68%). Peripheral blood stem cells were the graft source for 50% of the recipients. The second rectosigmoid biopsy performed for evaluation of steroid-refractory aGVHD occurred at a median of 19 days (interquartile range [IQR] 12-49 days) after the first biopsy. Seventeen patients received antithymocyte globulin as second line therapy in the cohort; the remaining 5 patients received etanercept as their second line therapy. Eighteen of 22 patients (82%) in this steroid-refractory GI aGVHD cohort died at a median 82.5 days (IQR 50 – 160 days) from the first rectosigmoid biopsy, with the majority of patients dying from GVHD (59%).

Differential Expression of Single Genes

We show the overall structure of the dataset as demonstrated by principal components analysis of RNA sequencing and the nCounter® Human Immunology Panel in Figure 1A and 1B respectively. Overall, the normal samples tended to cluster together, with no clear pattern in the data structure when comparing onset versus steroid-refractory GI GVHD biopsies.

Several immune- and damage-relevant genes differed between aGVHD onset and normal samples in single gene analyses detailed in Table 2. The mostly highly differentially expressed gene in aGVHD compared to normal was chitinase 3-L-1 (*CHI3L1*, fold-change 3.4, adjusted p=0.003), a recently described antigenic target in Crohn's disease.(9) The most significantly decreased gene in aGVHD compared to

normal was aquaporin-8 (*AQP8*, fold change -5.0, adjusted p<0.001), a water channel with decreased expression in inflammatory bowel disease.(10) Comparing onset aGVHD versus steroid-refractory aGVHD in paired analyses, several RNA-related and MT genes were increased, while chemokine (C-C motif) ligand 18 (*CCL18*) and intelectin-1 (*ITLN1*) were decreased (Table 3). Descriptions of the functions of the top 25 up- and down-regulated genes with annotations summarized from RefSeq (11) are detailed in Tables 2 and 3.

In supervised analyses of immune checkpoint genes that can inhibit aGVHD, we found a significant increase in *IDO1* and *PDL1* at the onset of aGVHD that was subsequently lost in the steroid refractory setting (Figure 2), both validated with NanoString. We attempted but could not identify *PDL1* expression at the protein level in either aGVHD or normal GI tissue using the antibody in clinical use for solid tumors (Supplemental Figure 1). We found a similar pattern of increased gene expression of T cell immunoreceptor with Ig and ITIM domains (*TIGIT*) at the onset of aGVHD that significantly decreased in refractory aGVHD (only accessible for analysis using NanoString).

Relevant to potential interaction of host mucosa with microbiota, we found a significant increase in aryl hydrocarbon receptor (*AhR*) gene expression at aGVHD onset that was also elevated in the steroid-refractory setting, validated by NanoString (Figure 2). Similarly, we found that AREG expression was significantly higher in onset and steroid-refractory aGVHD compared to normal rectosigmoid biopsies, although there was no difference between the GVHD groups (Figure 2, AREG only accessible for analysis by RNAseq).

Gene Set Enrichment Analysis

We compared gene sets using the hallmark (H), curated (C2) and immunologic signature (C7) gene sets from the MSigDB collections to determine whether previously described gene sets could distinguish between the groups of biopsies. Figure 3A shows a heatmap of top differentially expressed genes within

these datasets. Mitochondrial gene *HMGCS2* was most significantly downregulated whereas *SETD7* was the most highly upregulated in aGVHD onset compared to normals. The top gene set increased in aGVHD was GSE8835, indicating changes in gene expression of T cells (Figure 3B), consistent with known aGVHD pathophysiology. However, GSEA showed no pathways that were statistically significantly different between onset versus steroid-refractory GI aGVHD, with the heatmap of the top differentially expressed genes showing less distinct boundaries (Figure 3C).

Enrichr Analysis

The Enrichr analysis of the top 25 increased genes in aGVHD compared to normal is located at http://amp.pharm.mssm.edu/Enrichr/enrich?dataset=48mwo, and the top 25 decreased genes is located at http://amp.pharm.mssm.edu/Enrichr/enrich?dataset=48mwq. The most highly enriched gene ontology biological process in aGVHD samples was inflammatory response (GO:0006954, $p<0.001$), consistent with the known pathophysiology of aGVHD. The most enriched biological process based upon decreased gene expression aGVHD was positive regulation of respiratory burst (GO:0060267, $p<0.001$).

Biological processes differing between onset and steroid-refractory aGVHD based upon the top 25 increased and decreased genes are located at http://amp.pharm.mssm.edu/Enrichr/enrich?dataset=48mwc and http://amp.pharm.mssm.edu/Enrichr/enrich?dataset=48mwk respectively and summarized in Figure 4. We observed that multiple biological processes involving metallothioneines (MT) were significantly increased, whereas the only process that was significantly decreased in steroid refractory GI aGVHD was regulation of T-cell apoptosis (GO:0070234), related to decreased expression of *IDO1* and *PDL1* in the steroid-refractory state (Table 4).

Cell Deconvolution Analysis

Using CIBERSORT to estimate cell composition, we observed more CD4+ activated memory T cells and M0 macrophages in onset GI aGVHD compared to normal rectosigmoid biopsies (Figure 5), consistent with known aGVHD pathophysiology. Both onset and steroid-refractory aGVHD had increased M1 macrophages compared to normal. However, M2 macrophages were the highest in steroid-refractory GI aGVHD compared to both aGVHD onset and normal biopsies. Plasma cells were also enriched in steroid-refractory aGVHD compared to aGVHD onset. We observed no differences in activated T-cell subsets between onset and steroid-refractory aGVHD. Resting CD4+ memory T cells and memory B cells were lower in onset and steroid-refractory aGVHD compared to controls. Resting mast cells were lower in steroid-refractory aGVHD compared to normal. Other comparisons did not reach statistical significance.

Association of gene expression with early mortality

Survival time after diagnosis of aGVHD is the most important clinical outcome. We sought to identify a gene expression pattern suggestive of early mortality by comparing differential gene expression in patients' survival above and below the median of 82.5 days. We found those patients with an early death higher expression of 4 genes: glycerol kinase (*GK*), phosphoglycerate kinase 1 pseudogene 2 (*PGK1P2*), histone cluster 1 H1 family member (*HIST1H1A*), and cytochrome C oxidase subunit 7B pseudogene 2 (*COX7BP2*, Figure 6). Based upon cell signaling analysis by Enrichr®, these genes indicate a greater degree of DNA damage and stress in patients with poor survival (Supplemental Figure 2). Patients with survival above the median generally had higher expression of genes (Figure 6) associated with activation of *Smoothened* (*SMO*, Supplemental Figure 3, p=0.005, q=0.04), a Hedgehog pathway gene shown to constrain damage due to colitis in a preclinical model.(12)

We also explored microbial sequences using PathSeq (13) in order to determine if there was a microbial pattern at aGVHD onset that was associated with early mortality. This approach subtracts

potential microbial genes from the human sequences for estimation of candidate microbes within whole genome sequencing data. We identified the top 10 microbes with the greatest differences between the 2 groups based on survival time. In unsupervised hierarchical clustering of these top 10 candidate microbes, we observed that the majority of patients with poor survival have low presence of candidate microbes compared to those with longer survival (Figure 7). This suggests a loss of mucosal microbes in general, as opposed to a pattern of differing microbial species, may be relevant to survival in aGVHD.

Discussion

Multiple T-cell independent mechanisms contribute to the pathophysiology of steroid-refractory aGVHD. Our results suggest that steroid-refractory aGVHD may be characterized by loss of host tissue tolerance signals, increased stress-induced MT expression, and accumulation of M2 macrophages and plasma cells. Early death is associated with higher expression of genes related to DNA damage at the onset of aGVHD, whereas prolonged survival may be associated with modulation of the Hedgehog pathway via *Smoothened*. These novel findings broaden the horizon for clinical investigation into a fatal disease. Notably, we did not identify significant differences in T-cell content in onset versus steroid-refractory aGVHD. Our data are consistent with a recently described mouse model of steroid-refractory aGVHD that did not show differences in donor T-cell driven inflammation.(14) Despite the lower quality input RNA from FFPE, our RNAseq results could be validated by NanoString®, a platform well suited for robust gene expression analysis in FFPE clinical samples.(15)

We made several novel observations comparing aGVHD onset to normal biopsies in this analysis. For example, we observed a significant elevation of *CHI3L1*, also known as *YKL-40*, a pro-inflammatory factor known pathogenic roles in neovascularization, macrophage recruitment, and bacterial adhesion, in aGVHD.(16-19) The potential role of *CHI3L1* in clinical allogeneic HCT has otherwise not been described aside from a report identifying elevated plasma CHI3L1 in transplant recipients with a very high HCT

comorbidity index of 5+.(20) Increased *CHI3L1* may suggest a longer duration of inflammation in aGVHD. In mice, *CHI3L1* expression is increased the most during the chronic phase of colitis where it functions to promote intestinal epithelial cell proliferation and survival.(21) On the other hand, CHI3L1 may worsen outcomes of aGVHD by facilitating bacterial adhesion to colonic epithelial cells, and possibly even serving as a neutrophilic antigenic target as recently described in Crohn's disease.(9, 22) Fecal *CHI3L1* can be quantified, and its concentration is closely associated with mucosal damage in inflammatory bowel disease.(23) Recently, Li et al described that knockout of *CHI3L1* in donor T cells increased aGVHD lethality in a murine model.(24) Our results may not be comparable as our study was not limited to isolating T cell effects. Nonetheless, future GVHD models should further delineate the role of *CHI3L1* expression in host intestinal epithelial cells, and its potential role as an alloantigen in aGVHD should be explored.

Our analysis also identified 5-fold decreased gene expression of AQP8 at the onset of aGVHD. *AQP8* is a water channel important for hydrogen peroxide transport and mitochondrial function known to be decreased in inflammatory bowel disease (IBD), suggesting additional molecular parallels between the inflammatory conditions of aGVHD and IBD.(10, 25-27) In our gene set enrichment analysis, an additional mitochondrial gene, *HMGCS2*, was significantly lower in aGVHD compared to controls. In rats, expression of *HCGCS2* is dependent upon microbiota-derived butyrate.(28) Although this relationship is not yet established in humans, the role of loss of butyrate as the major microbiota-derived energy source for enterocytes in aGVHD pathogenesis is of intense interest.(29) These findings regarding *AQP8* and *HMGCS2*, along with our findings of lower microbial RNA in patients with early mortality, suggest that fatal aGVHD may be associated with mitochondriopathy related at least in part to dysbiosis. Indeed, a critical role of butyrate improving mitochondrial respiration and preventing autophagy in colonocytes has been identified.(30) A recent large scale RNAseq analysis of over 600 patients with ulcerative colitis also indicated reduced mitochrondrial energy function along with shifts microbial community structures.(31)

Further functional studies will be necessary to confirm this potential microbiota-mitochondrial crosstalk in aGVHD.

A major strength of this study is paired analyses in patients at diagnosis of aGVHD compared to when they became steroid refractory. We observed that processes involved in MT-associated stress responses are increased in steroid-refractory aGVHD compared to aGVHD onset. MTs are widely expressed stress response proteins that bind heavy divalent metals and mitigate oxidative stress.(32) MT-positive cells can be observed infiltrating the lamina propria in patients with inflammatory and infectious colitis, with the number of MT-positive cells correlated with the severity of colitis.(33) Anti-MT antibodies have been developed for use in mouse models of IBD and represent a potential novel therapeutic target for patients.(34) It cannot be concluded from our analysis that an increase in MT gene expression is solely linked to stress, as glucocorticoid exposure can also induce MT gene expression, thus possibly indicating a treatment effect in these biopsies.(35)

Beyond inflammation, steroid-refractory versus onset aGVHD appears to be associated with a tissue repair response with increased *AhR, AREG,* and *SETD7* expression. AhR activation is protective in colitis by regulating intestinal crypt stem cell differentiation.(36) AhR signaling can also drive immune responses in favor of either regulatory T cell or Th17 differentiation, suggesting ligand- and cell type-specific effects that could either ameliorate or worsen aGVHD.(37, 38) AREG is similarly protective in models of colitis and associated with Treg- and T9-mediated tissue repair.(39-43) AREG protein expression in the GI tract during clinical aGVHD can be variable, and the prognosis is largely driven by whether AREG is found in the circulation (unfavorable) or not (favorable).(44, 45) *SETD7*, the most highly differentially expressed gene comparing onset aGVHD to normal biopsies in our GSEA, is required for Wnt-dependent intestinal regeneration in chemical- or irradiation-induced damage.(46) Overall, an increase in expression

of *AhR*, *AREG*, and *SETD7* likely represent molecular processes supporting mucosal restitution after damage, although an increase in these genes did not lead to improved clinical outcomes in these patients.

One possible explanation for a failure of mucosal healing could be decreased expression of immune checkpoint genes, including *IDO1*, *PDL1*, and *TIGIT*. However, it is also possible that this observation is due to low interferon gamma related to low T cell content, but this cannot be conclusively determined through RNAseq. Previous studies have shown an increase in *IDO1* expression in the setting of aGVHD.(47, 48) Our results are consistent with these reports and extend these findings by demonstrating that *IDO1* expression decreases when patients transition to the steroid-refractory state. Similarly, PDL1 expression can be increased in colonic epithelium in the setting of inflammation, and its loss on host tissues is associated with poorer outcomes due to increased gut T cell homing, impaired T cell apoptosis, and impaired IL-22 production from CD11c+CD11b+ lamina propria cells.(49, 50) TIGIT is involved in regulating experimental aGVHD, with TIGIT-Fc attenuating aGVHD severity and T-cell TIGIT deficiency accelerating it.(51, 52) Identifying therapies that can sustain expression of inhibitory checkpoints may prove protective in life-threatening intestinal aGVHD.

Our analysis found that M2 macrophages but not T cells accumulated during steroid-refractory aGVHD. M2 macrophages have also shown to accumulate with chronicity in IBD and impair enterocyte differentiation through activation of Wnt signaling, suggesting their presence may indicate incomplete tissue repair.(53) Future functional and single-cell studies of the mucosal immune cells will be required to clarify the role of M2 macrophages in steroid-refractory aGVHD.

Our study is limited in that our findings cannot be validated using immunohistochemistry, as the samples were consumed during RNA extraction. Additionally, our analysis was on heterogeneous populations of cells, and subtle shifts within smaller immune cell populations may not be detectable. A large, independent data set with clinical samples adequate for both single cell sequencing and histology

will be necessary to validate these findings. Such a study may not be possible within single institutions due to small sample size and most patients not undergoing repeat diagnostic endoscopy in the setting of steroid-refractory aGVHD. Nonetheless, focused efforts designed to deconstruct the molecular mechanisms underlying steroid refractoriness in aGVHD should continue.

In summary, our analysis of the human mucosal aGVHD transcriptome expands the paradigm of T cell-centric therapies for steroid-refractory GI aGVHD. We have highlighted multiple new potential mechanisms for scientific investigation and therapeutic exploration for this fatal condition. Ultimately, multi-faceted and personalized approaches that support tolerance, enhance tissue repair, restore commensal microbiota, and improve mitochondrial function will be needed to reduce the substantial risk of mortality due to severe intestinal aGVHD.

Methods

All patients in this dataset underwent allogeneic HCT at the University of Minnesota between 2008-2016. We performed RNAseq on FFPE rectosigmoid biopsies from 22 adult patients with clinical stage 3-4 GI aGVHD at the onset of GI aGVHD, repeated at the diagnosis of steroid-refractory GI aGVHD. Rectosigmoid biopsies have 70% sensitivity, 87% specificity, and 97% positive predictive value for the diagnosis of aGVHD (54), therefore representing an excellent, consistent site of biopsy for RNA-seq analysis. All 22 patients had histologic evidence of GI aGVHD and did not have confounding infectious diagnoses (e.g., cytometgalovirus or concurrent C. difficile colitis). These patients were the only adult HCT recipients at our institution with stage 3-4 severity at onset of who underwent repeat biopsy and had FFPE blocks available for analysis at the time of the study. We compared these 22 paired GI aGVHD biopsies to FFPE rectosigmoid biopsies obtained from 10 healthy controls who had histologic analyses previously published.(44)

We extracted RNA from the FFPE biopsies using PureLink® FFPE RNA Isolation Kit (Thermo Fisher Scientific, Waltham, MA, USA). The entire biopsy was consumed in the process of RNA extraction. FFPE samples yielded an adequate quantity of RNA for sequencing (median 11,707 ng, range 290 – 33,220 ng), although as expected RNA integrity numbers (RIN) were low (median RIN 2.2, range 1.1 – 3.3). After extraction, we prepared the libraries for analysis with the SMARTer® Stranded Total RNA kit (Takara Bio, Mountain View, CA) and performed sequencing using the Illumina HiSeq 2500® platform, high-output mode, paired-end reads, 50 cycles. For validation of key immunologic findings, we analyzed residual RNA using the nCounter® Human Immunology panel (NanoString, Seattle, WA).

We aligned and assembled sequences using TopHat and Cufflinks respectively, performed gene set enrichment analysis (GSEA) using MySigDB gene sets in GSEA v3.0®, analyzed pathways using Enrichr®, and estimated immune cell composition using CIBERSORT®. For estimation of microbial RNA content, we analyzed reads that were not mapped to the human genome. Specifically, we used hisat—un-conc-gz to output unmapped pair ends FASTQ files, then we aligned unmapped pair ends using the hisat2 algorithm. We then used Pathseq as a mapping and taxonomic classification algorithm to estimate abundance of candidate microbes using read counts assigned to each organism.(13) This approach has previously been employed to assess mucosal dysbiosis in Crohn's disease.(55) The raw data for both RNASeq and PathSeq is available at the Gene Expression Omnibus at GSE134662. To assess PDL1 staining in colon biopsies, we performed staining in a single test case (rectosigmoid biopsy of aGVHD from a patient not in this cohort) and control case (normal colon biopsy from a patient not in this cohort) using Food and Drug Administration-approved antibody Ventana SP263 in the University of Minnesota Medical Center's clinical pathology laboratory according to manufacturer's instructions.

Statistics

We assessed the overall structure of the data using principal components analysis. We compared gene expression across groups adjusting for multiple comparisons with Bonferroni correction within the Limma package. Our single gene expression data set was large; many dependent variables could lead to significantly low p-values by chance [47]. Limma provided Bonferroni adjusted p-values in their contrast matrix, accounting for sample size and prior test statistics used in the appropriate design matrix. In hypothesis-driven analyses, we made comparisons between groups using the Wilcoxon rank sum test without correction for multiple comparisons. All p-values were 2 sided.

Study Approval

This study of previously archived biological specimens and data was approved by the University of Minnesota Institutional Review Board.

Author contributions:

Shernan G. Holtan: designed research studies, acquired and analyzed data, wrote the manuscript

Ashraf Shabaneh: designed research studies, analyzed data, and wrote the manuscript

Brian C. Betts: analyzed data, and wrote the manuscript

Armin Rashidi: analyzed data, and wrote the manuscript

Margaret L. MacMillan: analyzed data, and wrote the manuscript

Celalletin Ustun: analyzed data, and wrote the manuscript

Khalid Amin: acquired specimens, analyzed data, and wrote the manuscript

Byron P. Vaughn: acquired specimens, analyzed data, and wrote the manuscript

Justin Howard: acquired specimens, analyzed data, and wrote the manuscript

Alexander Khoruts: acquired specimens, analyzed data, and wrote the manuscript

Mukta Arora: analyzed data, and wrote the manuscript

Todd E. DeFor: analyzed data, and wrote the manuscript

Darrell Johnson: performed experiments, analyzed data, and wrote the manuscript

Angela Panoskaltsis-Mortari: analyzed data, and wrote the manuscript

Bruce R. Blazar: analyzed data, and wrote the manuscript

Daniel J. Weisdorf: analyzed data, and wrote the manuscript

Jinhua Wang: designed research studies, analyzed data, and wrote the manuscript

Acknowledgements:

This study was funded by the University of Minnesota Department of Medicine Women's Early Research Career program (SGH), 2 R01 HL56067 (BRB), and R37 AI34495 (BRB).

REFERENCES

1. Westin JR, Saliba RM, De Lima M, Alousi A, Hosing C, Qazilbash MH, Khouri IF, Shpall EJ, Anderlini P, Rondon G, et al. Steroid-Refractory Acute GVHD: Predictors and Outcomes. *Advances in hematology.* 2011;2011(601953.
2. Xhaard A, Rocha V, Bueno B, de Latour RP, Lenglet J, Petropoulou A, Rodriguez-Otero P, Ribaud P, Porcher R, Socie G, et al. Steroid-refractory acute GVHD: lack of long-term improved survival using new generation anticytokine treatment. *Biology of blood and marrow transplantation : journal of the American Society for Blood and Marrow Transplantation.* 2012;18(3):406-13.
3. Wall SA, Zhao Q, Yearsley M, Blower L, Agyeman A, Ranganathan P, Yang S, Wu H, Bostic M, Jaglowski S, et al. Complement-mediated thrombotic microangiopathy as a link between endothelial damage and steroid-refractory GVHD. *Blood advances.* 2018;2(20):2619-28.
4. Melson J, Jakate S, Fung H, Arai S, and Keshavarzian A. Crypt loss is a marker of clinical severity of acute gastrointestinal graft-versus-host disease. *Am J Hematol.* 2007;82(10):881-6.
5. da Costa LNG, Costa-Lima C, de Meirelles LR, Carvalho RB, Colella MP, Aranha FJP, Vigorito AC, and De Paula EV. Association between histopathological alterations and diarrhea severity in acute intestinal graft-versus-host disease. *Medicine.* 2018;97(19):e0600.
6. Martinez C, Rosales M, Calvo X, Cuatrecasas M, Rodriguez-Carunchio L, Llach J, Fernandez-Aviles F, Rosinol L, Rovira M, Carreras E, et al. Serial intestinal endoscopic examinations of patients with persistent diarrhea after allo-SCT. *Bone Marrow Transplant.* 2012;47(5):694-9.
7. Westermann AJ, and Vogel J. Host-Pathogen Transcriptomics by Dual RNA-Seq. *Methods Mol Biol.* 2018;1737(59-75.
8. Marsh JW, Hayward RJ, Shetty AC, Mahurkar A, Humphrys MS, and Myers GSA. Bioinformatic analysis of bacteria and host cell dual RNA-sequencing experiments. *Brief Bioinform.* 2018;19(6):1115-29.
9. Deutschmann C, Sowa M, Murugaiyan J, Roesler U, Rober N, Conrad K, Laass M, Bogdanos D, Sipeki N, Papp M, et al. Identification of Chitinase-3-like protein 1 as a novel neutrophil antigenic target in Crohn's disease. *J Crohns Colitis.* 2019.
10. Ricanek P, Lunde LK, Frye SA, Stoen M, Nygard S, Morth JP, Rydning A, Vatn MH, Amiry-Moghaddam M, and Tonjum T. Reduced expression of aquaporins in human intestinal mucosa in early stage inflammatory bowel disease. *Clinical and experimental gastroenterology.* 2015;8(49-67.
11. RefSeq. *https://wwwncbinlmnihgov/refseq/.* 2019;Accessed March 25, 2019/(
12. Lee JJ, Rothenberg ME, Seeley ES, Zimdahl B, Kawano S, Lu WJ, Shin K, Sakata-Kato T, Chen JK, Diehn M, et al. Control of inflammation by stromal Hedgehog pathway activation restrains colitis. *Proc Natl Acad Sci U S A.* 2016;113(47):E7545-E53.
13. Kostic AD, Ojesina AI, Pedamallu CS, Jung J, Verhaak RG, Getz G, and Meyerson M. PathSeq: software to identify or discover microbes by deep sequencing of human tissue. *Nat Biotechnol.* 2011;29(5):393-6.
14. Toubai T, Rossi C, Tawara I, Liu C, Zajac C, Oravecz-Wilson K, Peltier D, Sun Y, Fujiwara H, Wu SR, et al. Murine Models of Steroid Refractory Graft-versus-Host Disease. *Scientific reports.* 2018;8(1):12475.
15. Veldman-Jones MH, Brant R, Rooney C, Geh C, Emery H, Harbron CG, Wappett M, Sharpe A, Dymond M, Barrett JC, et al. Evaluating Robustness and Sensitivity of the NanoString Technologies nCounter Platform to Enable Multiplexed Gene Expression Analysis of Clinical Samples. *Cancer Res.* 2015;75(13):2587-93.

16. Li TM, Liu SC, Huang YH, Huang CC, Hsu CJ, Tsai CH, Wang SW, and Tang CH. YKL-40-Induced Inhibition of miR-590-3p Promotes Interleukin-18 Expression and Angiogenesis of Endothelial Progenitor Cells. *International journal of molecular sciences.* 2017;18(5).
17. Rathcke CN, and Vestergaard H. YKL-40, a new inflammatory marker with relation to insulin resistance and with a role in endothelial dysfunction and atherosclerosis. *Inflammation research : official journal of the European Histamine Research Society [et al].* 2006;55(6):221-7.
18. Kawada M, Chen CC, Arihiro A, Nagatani K, Watanabe T, and Mizoguchi E. Chitinase 3-like-1 enhances bacterial adhesion to colonic epithelial cells through the interaction with bacterial chitin-binding protein. *Laboratory investigation; a journal of technical methods and pathology.* 2008;88(8):883-95.
19. Tran HT, Lee IA, Low D, Kamba A, Mizoguchi A, Shi HN, Lee CG, Elias JA, and Mizoguchi E. Chitinase 3-like 1 synergistically activates IL6-mediated STAT3 phosphorylation in intestinal epithelial cells in murine models of infectious colitis. *Inflammatory bowel diseases.* 2014;20(5):835-46.
20. Kornblit B, Wang T, Lee SJ, Spellman SR, Zhu X, Fleischhauer K, Muller C, Verneris MR, Muller K, Johansen JS, et al. YKL-40 in allogeneic hematopoietic cell transplantation after AML and myelodysplastic syndrome. *Bone Marrow Transplant.* 2016;51(12):1556-60.
21. Low D, Subramaniam R, Lin L, Aomatsu T, Mizoguchi A, Ng A, DeGruttola AK, Lee CG, Elias JA, Andoh A, et al. Chitinase 3-like 1 induces survival and proliferation of intestinal epithelial cells during chronic inflammation and colitis-associated cancer by regulating S100A9. *Oncotarget.* 2015;6(34):36535-50.
22. Mizoguchi E. Chitinase 3-like-1 exacerbates intestinal inflammation by enhancing bacterial adhesion and invasion in colonic epithelial cells. *Gastroenterology.* 2006;130(2):398-411.
23. Buisson A, Vazeille E, Minet-Quinard R, Goutte M, Bouvier D, Goutorbe F, Pereira B, Barnich N, and Bommelaer G. Faecal chitinase 3-like 1 is a reliable marker as accurate as faecal calprotectin in detecting endoscopic activity in adult patients with inflammatory bowel diseases. *Aliment Pharmacol Ther.* 2016;43(10):1069-79.
24. Li Z, Lu H, Gu J, Liu J, Zhu Q, Lu Y, and Wang X. Chitinase 3-Like-1-Deficient Splenocytes Deteriorated the Pathogenesis of Acute Graft-Versus-Host Disease via Regulating Differentiation of Tfh Cells. *Inflammation.* 2017;40(5):1576-88.
25. Calamita G, Ferri D, Gena P, Liquori GE, Cavalier A, Thomas D, and Svelto M. The inner mitochondrial membrane has aquaporin-8 water channels and is highly permeable to water. *The Journal of biological chemistry.* 2005;280(17):17149-53.
26. Zahn A, Moehle C, Langmann T, Ehehalt R, Autschbach F, Stremmel W, and Schmitz G. Aquaporin-8 expression is reduced in ileum and induced in colon of patients with ulcerative colitis. *World journal of gastroenterology.* 2007;13(11):1687-95.
27. Min M, Peng LH, Sun G, Guo MZ, Qiu ZW, and Yang YS. Aquaporin 8 expression is reduced and regulated by microRNAs in patients with ulcerative colitis. *Chinese medical journal.* 2013;126(8):1532-7.
28. Cherbuy C, Andrieux C, Honvo-Houeto E, Thomas M, Ide C, Druesne N, Chaumontet C, Darcy-Vrillon B, and Duee PH. Expression of mitochondrial HMGCoA synthase and glutaminase in the colonic mucosa is modulated by bacterial species. *Eur J Biochem.* 2004;271(1):87-95.
29. Mathewson ND, Jenq R, Mathew AV, Koenigsknecht M, Hanash A, Toubai T, Oravecz-Wilson K, Wu SR, Sun Y, Rossi C, et al. Gut microbiome-derived metabolites modulate intestinal epithelial cell damage and mitigate graft-versus-host disease. *Nat Immunol.* 2016;17(5):505-13.
30. Donohoe DR, Garge N, Zhang X, Sun W, O'Connell TM, Bunger MK, and Bultman SJ. The microbiome and butyrate regulate energy metabolism and autophagy in the mammalian colon. *Cell Metab.* 2011;13(5):517-26.

31. Haberman Y, Karns R, Dexheimer PJ, Schirmer M, Somekh J, Jurickova I, Braun T, Novak E, Bauman L, Collins MH, et al. Ulcerative colitis mucosal transcriptomes reveal mitochondriopathy and personalized mechanisms underlying disease severity and treatment response. *Nat Commun.* 2019;10(1):38.
32. Subramanian Vignesh K, and Deepe GS, Jr. Metallothioneins: Emerging Modulators in Immunity and Infection. *International journal of molecular sciences.* 2017;18(10).
33. Devisscher L, Hindryckx P, Lynes MA, Waeytens A, Cuvelier C, De Vos F, Vanhove C, Vos MD, and Laukens D. Role of metallothioneins as danger signals in the pathogenesis of colitis. *The Journal of pathology.* 2014;233(1):89-100.
34. Dostie KE, Thees AV, and Lynes MA. Metallothionein: a Novel Therapeutic Target for Treatment of Inflammatory Bowel Disease. *Current pharmaceutical design.* 2018.
35. Jacob ST, Ghoshal K, and Sheridan JF. Induction of metallothionein by stress and its molecular mechanisms. *Gene Expr.* 1999;7(4-6):301-10.
36. Metidji A, Omenetti S, Crotta S, Li Y, Nye E, Ross E, Li V, Maradana MR, Schiering C, and Stockinger B. The Environmental Sensor AHR Protects from Inflammatory Damage by Maintaining Intestinal Stem Cell Homeostasis and Barrier Integrity. *Immunity.* 2018;49(2):353-62 e5.
37. Dant TA, Lin KL, Bruce DW, Montgomery SA, Kolupaev OV, Bommiasamy H, Bixby LM, Woosley JT, McKinnon KP, Gonzalez FJ, et al. T-cell expression of AhR inhibits the maintenance of pTreg cells in the gastrointestinal tract in acute GVHD. *Blood.* 2017;130(3):348-59.
38. Veldhoen M, Hirota K, Westendorf AM, Buer J, Dumoutier L, Renauld JC, and Stockinger B. The aryl hydrocarbon receptor links TH17-cell-mediated autoimmunity to environmental toxins. *Nature.* 2008;453(7191):106-9.
39. Chen F, Yang W, Huang X, Cao AT, Bilotta AJ, Xiao Y, Sun M, Chen L, Ma C, Liu X, et al. Neutrophils Promote Amphiregulin Production in Intestinal Epithelial Cells through TGF-beta and Contribute to Intestinal Homeostasis. *J Immunol.* 2018;201(8):2492-501.
40. Monticelli LA, Osborne LC, Noti M, Tran SV, Zaiss DM, and Artis D. IL-33 promotes an innate immune pathway of intestinal tissue protection dependent on amphiregulin-EGFR interactions. *Proc Natl Acad Sci U S A.* 2015;112(34):10762-7.
41. Brandl K, Sun L, Neppl C, Siggs OM, Le Gall SM, Tomisato W, Li X, Du X, Maennel DN, Blobel CP, et al. MyD88 signaling in nonhematopoietic cells protects mice against induced colitis by regulating specific EGF receptor ligands. *Proc Natl Acad Sci U S A.* 2010;107(46):19967-72.
42. Arpaia N, Green JA, Moltedo B, Arvey A, Hemmers S, Yuan S, Treuting PM, and Rudensky AY. A Distinct Function of Regulatory T Cells in Tissue Protection. *Cell.* 2015;162(5):1078-89.
43. Ramadan A, Griesenauer B, Adom D, Kapur R, Hanenberg H, Liu C, Kaplan MH, and Paczesny S. Specifically differentiated T cell subset promotes tumor immunity over fatal immunity. *J Exp Med.* 2017;214(12):3577-96.
44. Amin K, Yaqoob U, Schultz B, Vaughn BP, Khoruts A, Howard JR, DeFor TE, Forster C, Meyer C, Gandhi I, et al. Amphiregulin in intestinal acute graft-versus-host disease: a possible diagnostic and prognostic aid. *Modern pathology : an official journal of the United States and Canadian Academy of Pathology, Inc.* 2018.
45. Holtan SG, DeFor TE, Panoskaltsis-Mortari A, Khera N, Levine JE, Flowers MED, Lee SJ, Inamoto Y, Chen GL, Mayer S, et al. Amphiregulin modifies the Minnesota Acute Graft-versus-Host Disease Risk Score: results from BMT CTN 0302/0802. *Blood Adv.* 2018;2(15):1882-8.
46. Oudhoff MJ, Braam MJS, Freeman SA, Wong D, Rattray DG, Wang J, Antignano F, Snyder K, Refaeli I, Hughes MR, et al. SETD7 Controls Intestinal Regeneration and Tumorigenesis by Regulating Wnt/beta-Catenin and Hippo/YAP Signaling. *Dev Cell.* 2016;37(1):47-57.

47. Jasperson LK, Bucher C, Panoskaltsis-Mortari A, Taylor PA, Mellor AL, Munn DH, and Blazar BR. Indoleamine 2,3-dioxygenase is a critical regulator of acute graft-versus-host disease lethality. *Blood.* 2008;111(6):3257-65.
48. Ratajczak P, Janin A, Peffault de Larour R, Koch L, Roche B, Munn D, Blazar BR, and Socie G. IDO in human gut graft-versus-host disease. *Biology of blood and marrow transplantation : journal of the American Society for Blood and Marrow Transplantation.* 2012;18(1):150-5.
49. Scandiuzzi L, Ghosh K, Hofmeyer KA, Abadi YM, Lazar-Molnar E, Lin EY, Liu Q, Jeon H, Almo SC, Chen L, et al. Tissue-expressed B7-H1 critically controls intestinal inflammation. *Cell reports.* 2014;6(4):625-32.
50. Saha A, Aoyama K, Taylor PA, Koehn BH, Veenstra RG, Panoskaltsis-Mortari A, Munn DH, Murphy WJ, Azuma M, Yagita H, et al. Host programmed death ligand 1 is dominant over programmed death ligand 2 expression in regulating graft-versus-host disease lethality. *Blood.* 2013;122(17):3062-73.
51. Yu X, Harden K, Gonzalez LC, Francesco M, Chiang E, Irving B, Tom I, Ivelja S, Refino CJ, Clark H, et al. The surface protein TIGIT suppresses T cell activation by promoting the generation of mature immunoregulatory dendritic cells. *Nat Immunol.* 2009;10(1):48-57.
52. Zhang D, Hu W, Xie J, Zhang Y, Zhou B, Liu X, Zhang Y, Su Y, Jin B, Guo S, et al. TIGIT-Fc alleviates acute graft-versus-host disease by suppressing CTL activation via promoting the generation of immunoregulatory dendritic cells. *Biochim Biophys Acta Mol Basis Dis.* 2018;1864(9 Pt B):3085-98.
53. Cosin-Roger J, Ortiz-Masia D, Calatayud S, Hernandez C, Alvarez A, Hinojosa J, Esplugues JV, and Barrachina MD. M2 macrophages activate WNT signaling pathway in epithelial cells: relevance in ulcerative colitis. *Plos One.* 2013;8(10):e78128.
54. Wild D, Sung AD, Cardona D, Cirricione C, Sullivan K, Detweiler C, Shealy M, Balmadrid B, Rowes KL, Chao N, et al. The Diagnostic Yield of Site and Symptom-Based Biopsies for Acute Gastrointestinal Graft-Versus-Host Disease: A 5-Year Retrospective Review. *Digestive diseases and sciences.* 2015.
55. Pedamallu CS, Bhatt AS, Bullman S, Fowler S, Freeman SS, Durand J, Jung J, Duke F, Manzo V, Cai D, et al. Metagenomic Characterization of Microbial Communities In Situ Within the Deeper Layers of the Ileum in Crohn's Disease. *Cell Mol Gastroenterol Hepatol.* 2016;2(5):563-6 e5.

Figure 1. Principal components analysis of the entire RNAseq dataset (A) and entire NanoString dataset (B).

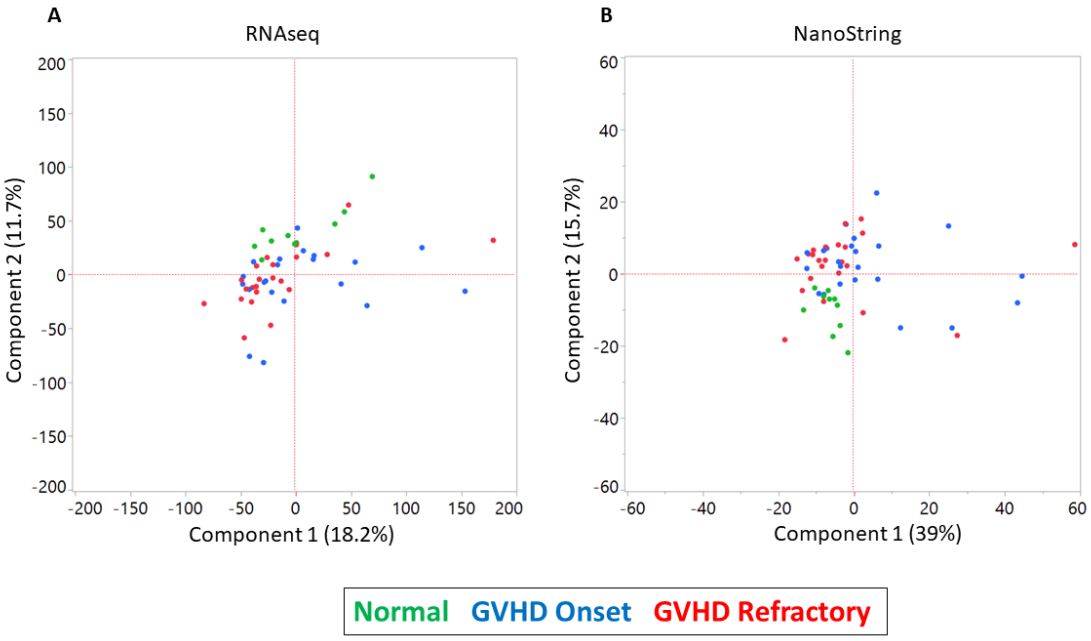

Figure 2. RNAseq (A) and NanoString (B) single gene analyses of programmed death ligand-1 (PDL1), aryl hydrocarbon receptor, indoleamine 2, 3 dioxygenase (IDO1), amphiregulin (AREG), and T cell immunoreceptor with Ig and ITIM domains (TIGIT). Boxplots show differences between groups (onset N=22, refractory N=22, and normal N=10), with medians compared by Wilcoxon rank sum test.

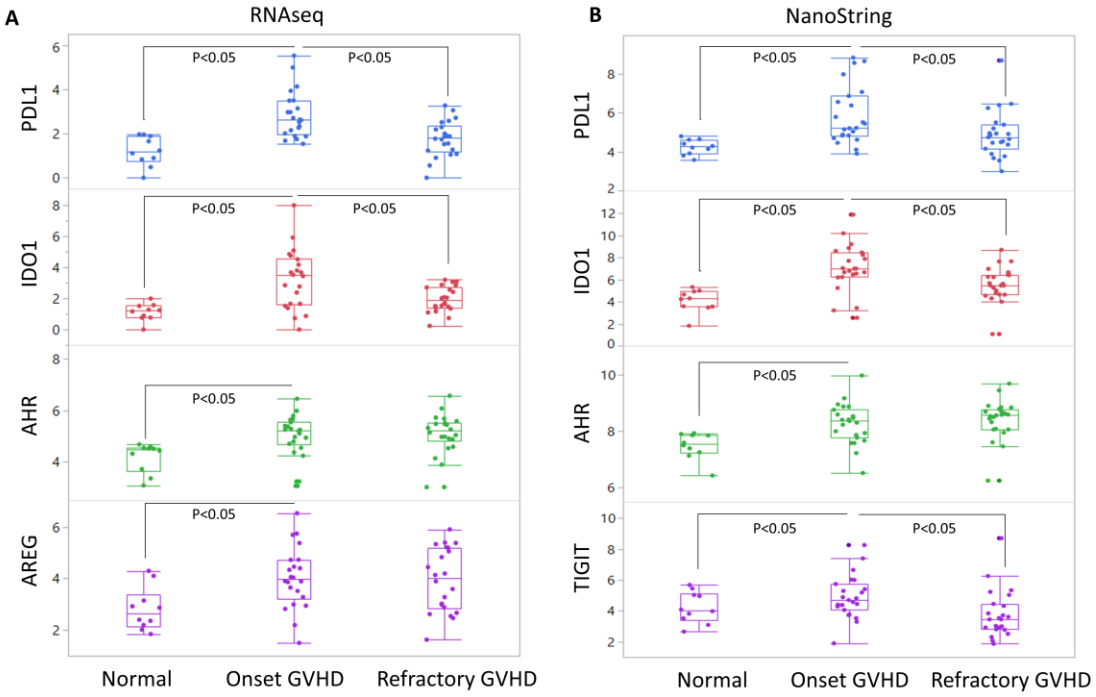

Figure 3. (A) Heatmap of differentially expressed genes in onset acute graft-versus-host disease (aGVHD) vs controls. (B) Enrichment plot of top expressed pathway in aGVHD vs controls.

A

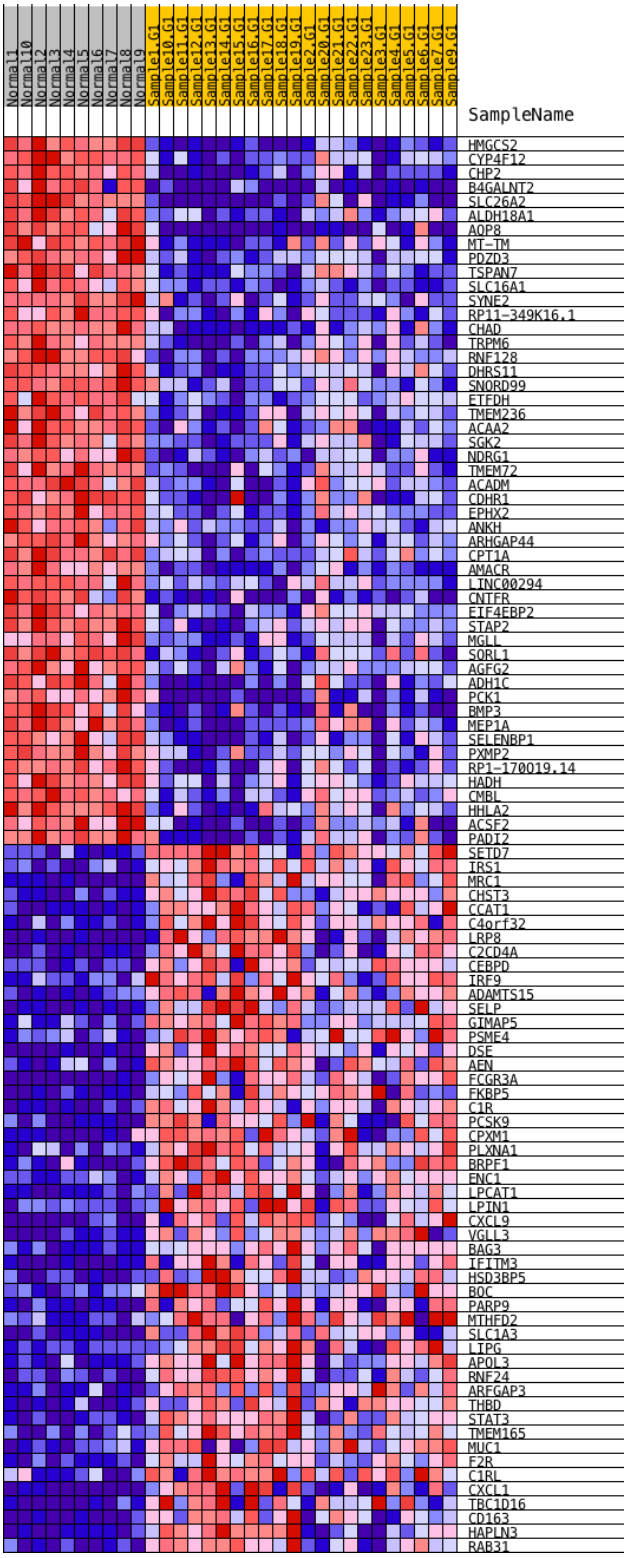

B

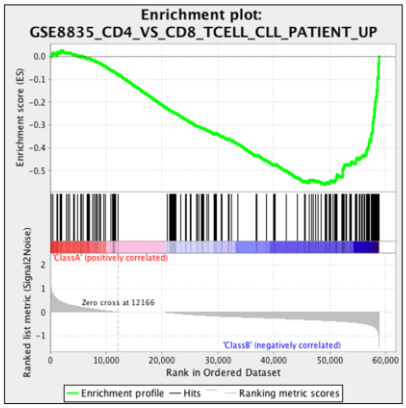

Normalized Enrichment Score	-2.0067735
Nominal p-value	0.0
FDR q-value	0.5925871
FWER p-Value	0.057

Figure 4. Gene ontology biological processes as determined by top 25 increased (A) and top 25 decreased (B) genes in onset versus steroid-refractory acute graft-versus-host disease (aGVHD). (C) heatmap of differentially expressed genes in onset vs steroid-refractory aGVHD.

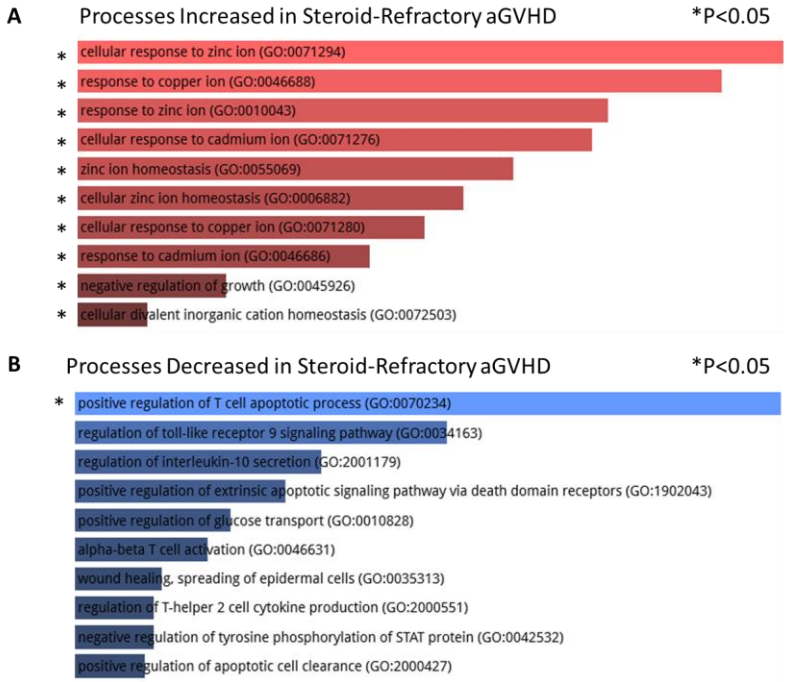

C

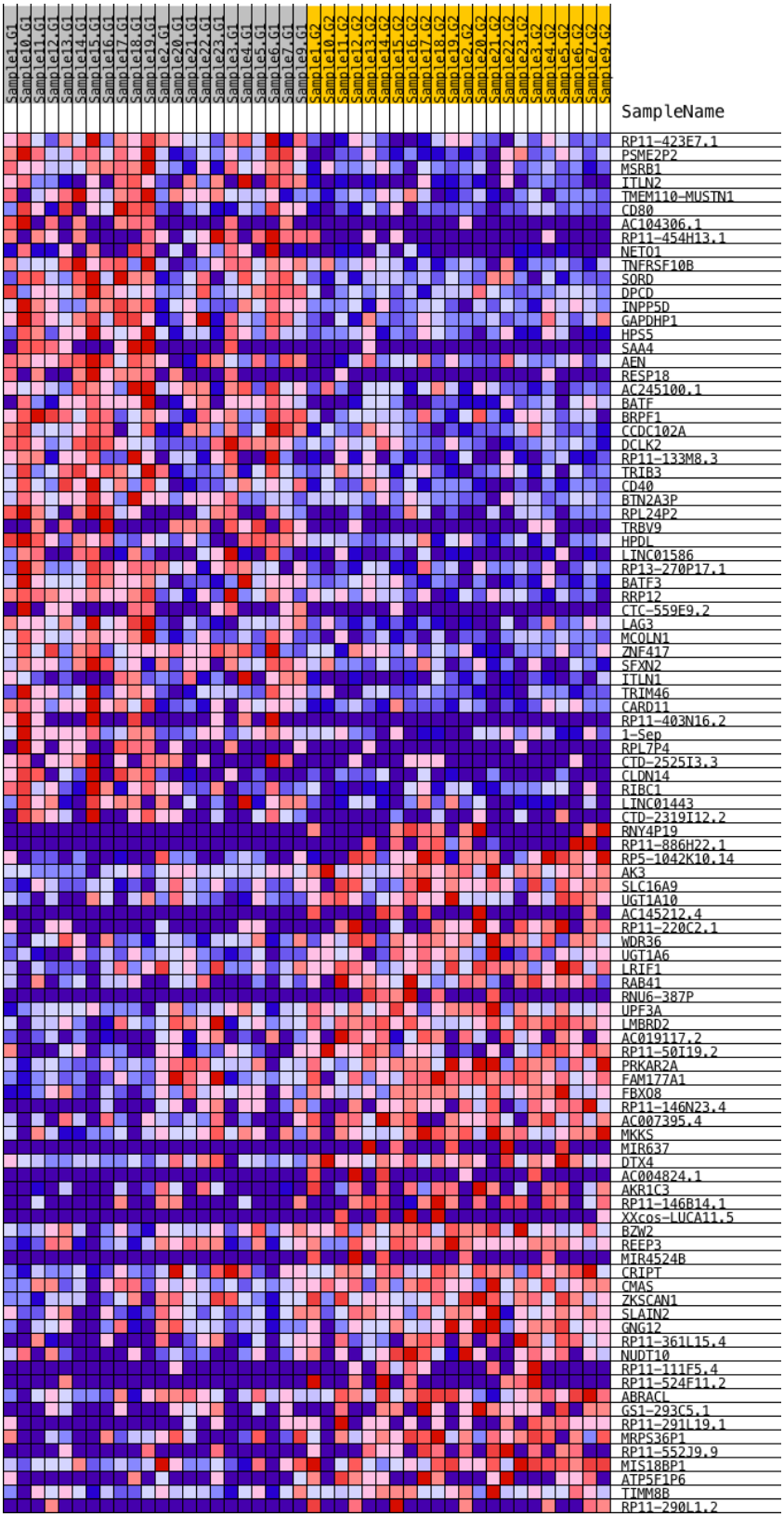
Sample1.G1
Sample10.G1
Sample11.G1
Sample12.G1
Sample13.G1
Sample14.G1
Sample15.G1
Sample16.G1
Sample17.G1
Sample18.G1
Sample19.G1
Sample2.G1
Sample20.G1
Sample21.G1
Sample22.G1
Sample23.G1
Sample3.G1
Sample4.G1
Sample5.G1
Sample6.G1
Sample7.G1
Sample9.G1
Sample1.G2
Sample10.G2
Sample11.G2
Sample12.G2
Sample13.G2
Sample14.G2
Sample15.G2
Sample16.G2
Sample17.G2
Sample18.G2
Sample19.G2
Sample2.G2
Sample20.G2
Sample21.G2
Sample22.G2
Sample23.G2
Sample3.G2
Sample4.G2
Sample5.G2
Sample6.G2
Sample7.G2
Sample9.G2
SampleName
RP11-423E7.1
PSME2P2
MSRB1
ITLN2
TMEM110-MUSTN1
CD80
AC104306.1
RP11-454H13.1
NETO1
TNFRSF10B
SORD
DPCD
INPP5D
GAPDHP1
HPS5
SAA4
AEN
RESP18
AC245100.1
BATF
BRPF1
CCDC102A
DCLK2
RP11-133M8.3
TRIB3
CD40
BTN2A3P
RPL24P2
TRBV9
HPDL
LINC01586
RP13-270P17.1
BATF3
RRP12
CTC-559E9.2
LAG3
MCOLN1
ZNF417
SFXN2
ITLN1
TRIM46
CARD11
RP11-403N16.2
1-Sep
RPL7P4
CTD-2525I3.3
CLDN14
RIBC1
LINC01443
CTD-2319I12.2
RNY4P19
RP11-886H22.1
RP5-1042K10.14
AK3
SLC16A9
UGT1A10
AC145212.4
RP11-220C2.1
WDR36
UGT1A6
LRIF1
RAB41
RNU6-387P
UPF3A
LMBRD2
AC019117.2
RP11-50I19.2
PRKAR2A
FAM177A1
FBXO8
RP11-146N23.4
AC007395.4
MKKS
MIR637
DTX4
AC004824.1
AKR1C3
RP11-146B14.1
XXcos-LUCA11.5
BZW2
REEP3
MIR4524B
CRIPT
CMAS
ZKSCAN1
SLAIN2
GNG12
RP11-361L15.4
NUDT10
RP11-111F5.4
RP11-524F11.2
ABRACL
GS1-293C5.1
RP11-291L19.1
MRPS36P1
RP11-552J9.9
MIS18BP1
ATP5F1P6
TIMM8B
RP11-290L1.2

Figure 5. Immune cell deconvolution results using CIBERSORT®. Contour plots show differences in distribution between groups (onset N=22, refractory N=22, and normal N=10), with differences in medians compared by Wilcoxon rank sum test.

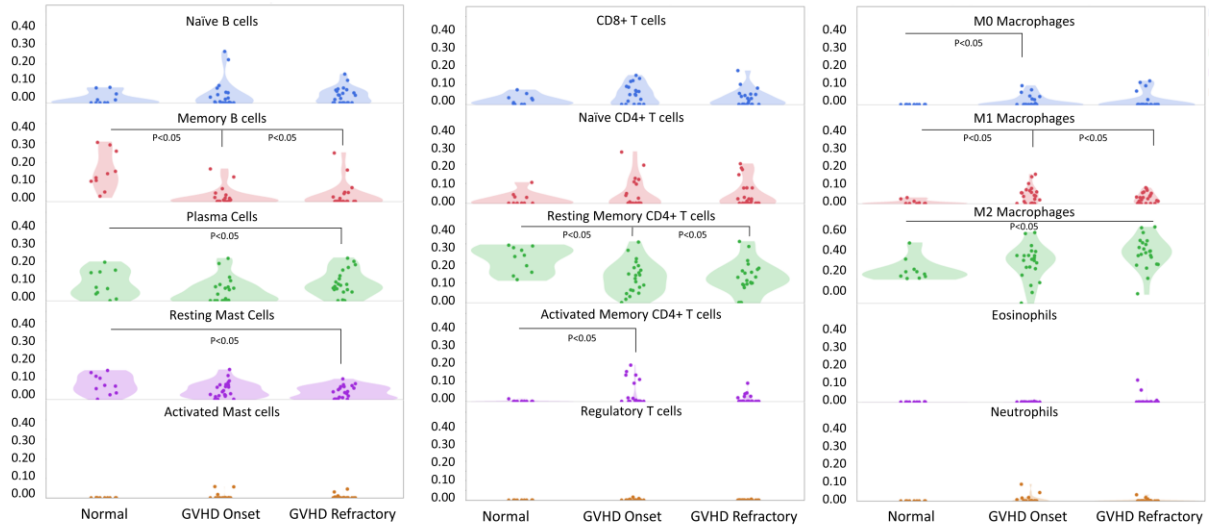

Figure 6. Unsupervised hierarchical cluster of top 10 genes differentiating early (<82.5 days) versus later (>82.5 days) death at acute graft-versus-host disease (aGVHD) onset. The top 10 genes comprise the rows, while individual patients and their survival time in days is indicated in the columns.

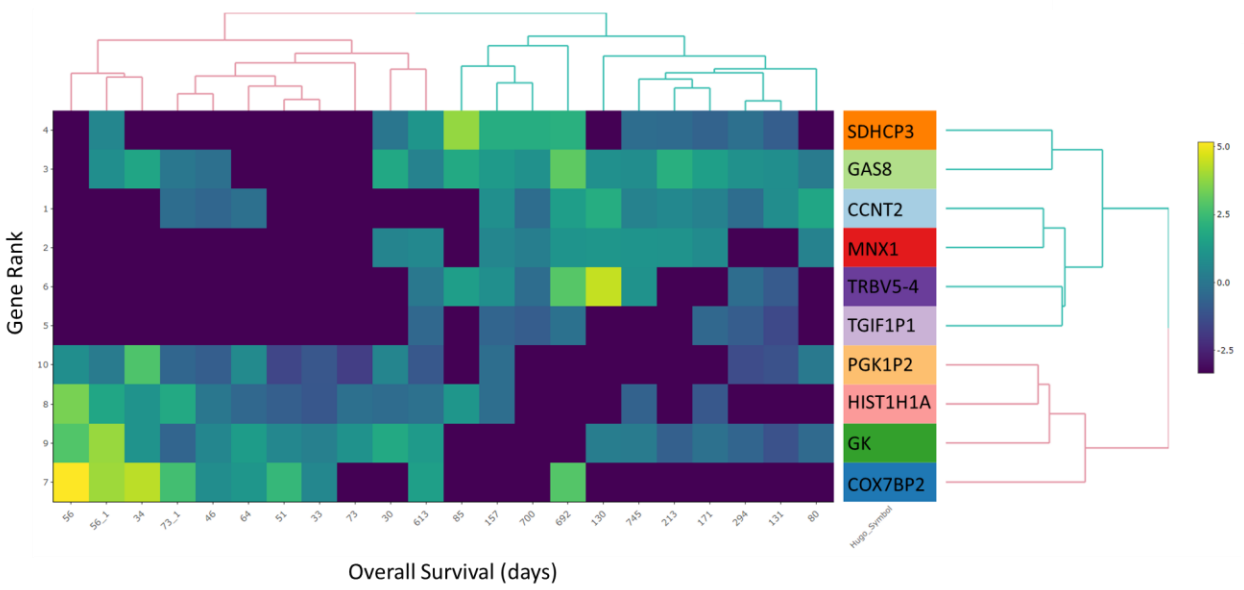

Figure 7. Unsupervised hierarchical cluster of predicted microbes differentiating early (<82.5 days) versus later (>82.5 days) death at acute graft-versus-host disease (aGVHD) onset. The top 10 microbes comprise the rows, while individual patients and their survival time in days is indicated in the columns.

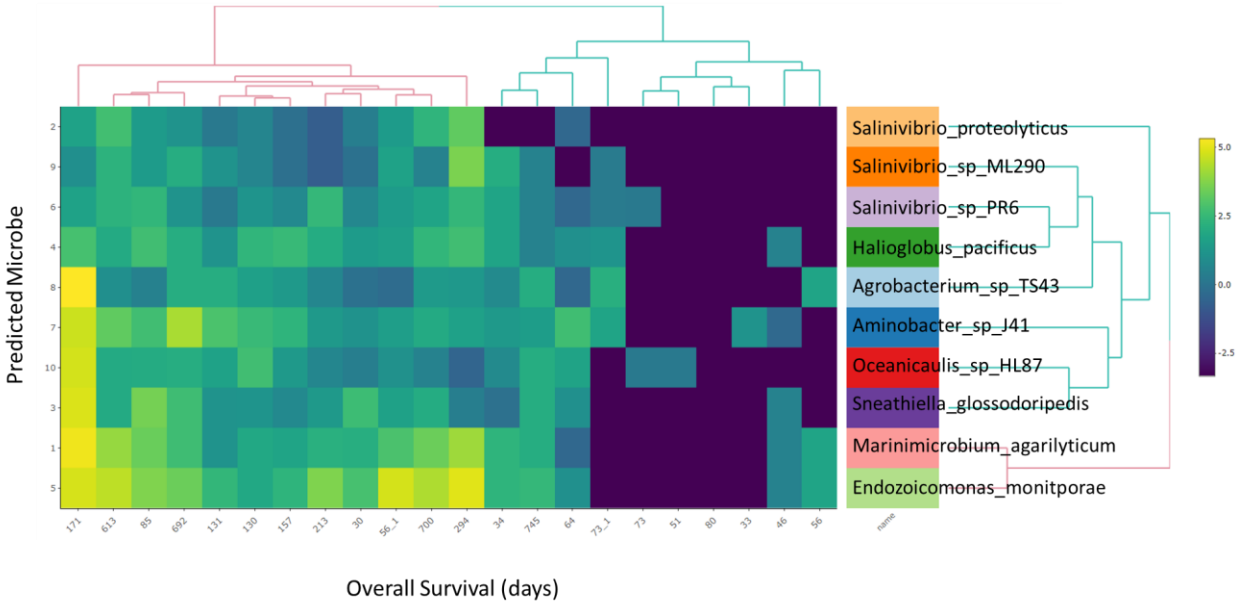

Table 1. Patient Demographics

Variable	N (%)
Gender	
Male	16 (73%)
Female	6 (27%)
Age (median, range)	49.8 years (20.4 – 68.9)
Diagnosis	
Acute myeloid leukemia	7 (32%)
Acute lymphoblastic leukemia	3 (14%)
Myelodysplastic syndrome	4 (18%)
Myeloproliferative neoplasms	3 (14%)
Lymphoma	3 (14%)
Multiple myeloma	2 (9%)
Graft Source	
Peripheral blood	11 (50%)
Bone marrow	3 (14%)
Umbilical cord blood	8 (36%)
Conditioning	
Myeloablative	7 (32%)
Reduced Intensity	15 (68%)
Cause of Death	
Alive	4 (18%)
GVHD	13 (59%)
Organ failure	2 (9%)
Infection	2 (9%)
Malignancy	1 (5%)
Days between first and second biopsy (median, interquartile range)	19 days (12 – 45)
Days between first biopsy and death (median, interquartile range)	82.5 days (56 – 202.5)

Table 2. Top 50 differentially expressed genes along with their principal protein functions from RefSeq (11) in onset GVHD versus normal colon.

NAME	Principal protein functions	Fold Change	Adjusted p
CHI3L1	Tissue remodeling, Th2 response, M2 differentiation, bacterial adhesion/invasion, mediates AKT1 signaling and IL-8 production in colonic epithelial cells.	3.39169	0.00284
CXCL1	Neutrophil chemoattractant	2.98659	0.00029
OLFM4	Antiapopotic factor expressed in inflamed colonic epithelium	2.93931	0.00630
FCGR3A	Receptor for the Fc portion of immunoglobulin G, involved in the removal of antigen-antibody complexes from the circulation	2.84701	0.00000
DUOX2	Member of the NADPH oxidase family	2.71736	0.02139
NNMT	N-methylation of drugs and xenobiotic compounds	2.60061	0.00004
CCL18	Attracts naive T lymphocytes toward dendritic cells and activated macrophages	2.55275	0.00159
TGM2	Transglutaminase, autoantigen implicated in celiac disease	2.54470	0.00006
UBD	Ubiquitin D, caspase-dependent apoptosis, formation of aggresomes, mitotic regulation, and dendritic cell maturation	2.49085	0.00665
RN7SL1	Cytoplasmic ribonucleoprotein complex that mediates cotranslational insertion of secretory proteins into the lumen of the endoplasmic reticulum	2.40793	0.25095
SERPINA3	Plasma protease inhibitor	2.36293	0.00004
SLC6A14	Transports both neutral and cationic amino acids	2.33822	0.00668
PDPN	Unknown; hysiological function of this protein may be related to its mucin-type character	2.32438	0.00027
LCN2	Plays a role in innate immunity by limiting bacterial growth as a result of sequestering iron-containing siderophores	2.32114	0.02528
PLA2G2A	Catalyzes the hydrolysis of the sn-2 fatty acid acyl ester bond of phosphoglycerides, releasing free fatty acids and lysophospholipids	2.29231	0.07601
RNU5A-8P	Pseudogene, snRNA class	2.27054	0.09680
IGFBP5	Insulin Like Growth Factor Binding Protein 5	2.21746	0.00331
CXCL3	Chemoattractant for neutrophils	2.18454	0.00126
PI3	Antimicrobial peptide against Gram-positive and Gram-negative bacteria, and fungal pathogens	2.18009	0.03881
GBP1	Guanylate binding protein expression, induced by interferon	2.17086	0.00028
IDO1	Through its expression in dendritic cells, monocytes, and macrophages, this enzyme modulates T-cell behavior by its peri-cellular catabolization of tryptophan	2.11768	0.00408
CXCL9	Chemoattractant for lymphocytes but not for neutrophils	2.11170	0.00020
GNLY	Granulysin, located in the cytotoxic granules of T cells, which are released upon antigen stimulation	2.10077	0.00806
AC073610.5	Unknown	2.08671	0.01301
SERPING1	Inhibits activated C1r and C1s of the first complement component and thus regulates complement activation	2.08552	0.00005

PADI2	Converts arginine residues into citrullines in the presence of calcium ions	-2.33776	0.00066
SNORA50A	snoRNA	-2.38652	0.14232
SELENBP1	Member of the selenium-binding protein family	-2.39655	0.00054
IGLC1	Immunoglobulin Lambda Constant 1, humoral immunity	-2.40012	0.12350
MT-TM	Mitochondrially Encoded TRNA Methionine	-2.42935	0.02513
SNORD14D	snoRNA	-2.43130	0.25825
IGKC	Immunoglobulin Kappa Constant, humoral immunity	-2.43859	0.14209
CA1	Carbonic anhydrase, catalyze the reversible hydration of carbon dioxide	-2.44360	0.05774
ADH1C	Class I alcohol dehydrogenase, gamma subunit	-2.56183	0.00061
IGHA1	Constant region of immunoglobulin heavy chains, humoral immunity	-2.57946	0.11866
SLC9A3	Epithelial brush border Na/H exchanger that uses an inward sodium ion gradient to expel acids from the cell; defects in this gene cause congenital secretory sodium diarrhea	-2.63871	0.00065
SCARNA10	Small Cajal Body-Specific RNA 10	-2.70487	0.16469
IGKV1-12	Immunoglobulin Kappa Variable 1-12, humoral immunity	-2.82150	0.02088
CHP2	Regulates cell pH by controlling plasma membrane-type Na+/H+ exchange activity	-2.88925	0.00005
IGHA2	Immunoglobulin Heavy Constant Alpha 2	-2.89415	0.06045
SNORD19	snoRNA	-2.99078	0.01352
SCARNA2	Small Cajal Body-Specific RNA 2	-3.01585	0.05952
B4GALNT2	Catalyzes the last step in the biosynthesis of the human Sd(a) antigen	-3.11747	0.00000
JCHAIN	Joining Chain Of Multimeric IgA And IgM	-3.29490	0.02117
PCK1	Main control point for the regulation of gluconeogenesis	-3.41424	0.00016
CD177	Bind platelet endothelial cell adhesion molecule-1 and function in neutrophil transmigration	-3.45107	0.00012
HMGCS2	Mitochondrial enzyme that catalyzes the first reaction of ketogenesis	-3.45173	0.00000
SLC26A2	Solute Carrier Family 26 Member 2	-3.59968	0.00001
SCARNA4	Small Cajal Body-Specific RNA 4	-4.90290	0.02708
AQP8	Water channel protein. Aquaporin 8 mRNA is found in pancreas and colon but not other tissues	-5.05477	0.00000

Table 3. Top 50 differentially expressed genes along with their principal protein functions from RefSeq (11) between onset and steroid-refractory GVHD.

NAME	Principal function	Fold Change	p-value (paired)
AC091053.2	Unknown	2.57153	0.00165
SCARNA4	Small Cajal Body-Specific RNA 4	2.36412	0.03078
MT1G	Metallothionein G, high content of cysteine residues that bind various heavy metals	2.29843	0.00026
MT-TR	Mitochondrially Encoded TRNA Arginine	1.85103	0.01231
SNORD19	snoRNA	1.78778	0.00550
RP11-361L15.4	RNA gene	1.60518	0.00095
SNORD101	snoRNA	1.56110	0.05140
MT1H	Metallothionein H, high content of cysteine residues that bind various heavy metals	1.51662	0.00536
SNORD121B	snoRNA	1.39516	0.03296
RP5-1042K10.14	RNA gene	1.28920	0.00008
SPINK4	Serine Peptidase Inhibitor, Kazal Type 4	1.26217	0.04338
RNY4	RNA, Ro-Associated Y4	1.24491	0.07367
MT-TV	Mitochondrially Encoded TRNA Valine	1.24042	0.11710
MT1M	Metallothionein M, high content of cysteine residues that bind various heavy metals	1.22836	0.00150
SNORD116-22	snoRNA	1.21861	0.05104
SNORD63	snoRNA	1.21342	0.07239
SNORD34	snoRNA	1.20635	0.05692
MT1F	Metallothionein F, high content of cysteine residues that bind various heavy metals	1.19965	0.02188
ADH1C	Class I alcohol dehydrogenase, gamma subunit	1.17598	0.00630
SNORD72	snoRNA	1.15740	0.03111
SNORD56	snoRNA	1.15373	0.07627
MIR1248	MIR1248	1.13942	0.07986
MT-TG	Mitochondrially Encoded TRNA Glycine	1.13098	0.06903
MT-TI	Mitochondrially Encoded TRNA Isoleucine	1.10760	0.06596
RNY3	RNA, Ro-Associated Y3	1.09840	0.07192
ATF3	Mammalian activation transcription factor/cAMP responsive element-binding (CREB) protein family of transcription factors	-1.05713	0.00132
G0S2	G0/G1 Switch 2	-1.05820	0.00677
RN7SL5P	RNA, 7SL, Cytoplasmic 5, Pseudogene	-1.06039	0.13184
ZAP70	Enzyme phosphorylated on tyrosine residues upon T-cell antigen receptor (TCR) stimulation, functions in the initial step of TCR-mediated signal transduction in combination with the Src family kinases, Lck and Fyn.	-1.06856	0.00003

NOS2	Nitric Oxide Synthase 2	-1.07029	0.03360
CD274 (PDL1)	Programmed death ligand 1. During infection or inflammation of normal tissue, this interaction is important for preventing autoimmunity by maintaining homeostasis of the immune response.	-1.07718	0.00100
C3	Complement 3; plays a central role in the activation of complement system. Its activation is required for both classical and alternative complement activation pathways	-1.07906	0.00005
RP11-326C3.2	Unknown	-1.08815	0.00354
DNASE1L3	Hydrolyzes DNA, is not inhibited by actin, and mediates the breakdown of DNA during apoptosis	-1.10131	0.00131
NKG7	Natural Killer Cell Granule Protein 7	-1.10767	0.00066
SNORD30	snoRNA	-1.16564	0.03575
TNIP3	TNFAIP3 Interacting Protein 3, involved in IL-23 signaling pathway	-1.16649	0.00235
ITGAX	Adherence of neutrophils and monocytes to stimulated endothelium cells	-1.18035	0.00026
RNA5SP514	RNA, 5S Ribosomal Pseudogene 514	-1.23535	0.02674
AL450304.2	Unknown	-1.23582	0.14966
RSAD2	Antiviral protein which plays a major role in the cell antiviral state induced by type I and type II interferon	-1.24246	0.00347
SOCS3	Suppressor Of Cytokine Signaling 3, involved in negative regulation of cytokines that signal through the JAK/STAT pathway	-1.25443	0.00014
UBD	Ubiquitin D, caspase-dependent apoptosis, formation of aggresomes, mitotic regulation, and dendritic cell maturation	-1.27289	0.01468
MMP12	Matrix Metalloproteinase 12 (Macrophage Elastase)	-1.28171	0.00166
AC009133.15	Unknown	-1.28343	0.00300
SLC7A5P2	Solute Carrier Family 7 Member 5 Pseudogene 2	-1.28583	0.00239
IDO1	Through its expression in dendritic cells, monocytes, and macrophages, this enzyme modulates T-cell behavior by its peri-cellular catabolization of tryptophan	-1.29182	0.00487
TNFRSF6B	Postulated to play a regulatory role in suppressing FasL- and LIGHT-mediated cell death	-1.43346	0.00044
CCL18	Chemotactic activity for naive T cells, CD4+ and CD8+ T cells and nonactivated lymphocytes, but not for monocytes or granulocytes	-1.55402	0.00007
ITLN1	Intelectin 1, probably plays a role in the defense against microorganisms.	-1.58999	0.02574

Table 4. Top gene ontology (GO) biological processes differentiating onset acute graft-versus-host disease (aGVHD) versus steroid-refractory aGVHD.

Top GO INCREASED in Steroid-Refractory aGVHD	**Adjusted P-value**	**Genes**
cellular response to zinc ion (GO:0071294)	1.23083E-07	MT1M;MT1F;MT1G;MT1H
cellular response to cadmium ion (GO:0071276)	1.70547E-07	MT1M;MT1F;MT1G;MT1H
cellular response to copper ion (GO:0071280)	1.23083E-07	MT1M;MT1F;MT1G;MT1H
negative regulation of growth (GO:0045926)	2.19211E-05	MT1M;MT1F;MT1G;MT1H
Top GO DECREASED in Steroid-Refractory aGVHD	**Adjusted P-value**	**Genes**
positive regulation of T cell apoptotic process (GO:0070234)	0.02	CD274 (PDL1); IDO1
positive regulation of glucose transport (GO:0010828)	0.06	C3;ITLN1
response to lipopolysaccharide (GO:0032496)	0.06	CD274 (PDL1);TNFRSF6B;TNIP3
cytokine-mediated signaling pathway (GO:0019221)	0.06	SOCS3;TNFRSF6B;RSAD2; ITGAX;CCL18